

Theory of sub-Doppler cooling of three-level Λ atoms in standing light waves

D. V. Kosachev and Yu. V. Rozhdestvenskii

St. Petersburg State Technical University, 195251 St. Petersburg, Russia

(Submitted 12 July 1994)

Zh. Eksp. Teor. Fiz. **106**, 1588–1605 (December 1994)

A general theory of cooling of three-level Λ atoms in two standing light waves between which there is a relative spatial phase shift is presented for arbitrary ratios of the intensity and detuning. It is shown that in the case of equal detuning of the light waves, deep (sub-Doppler) cooling of three-level atoms occurs for any values of the spatial phase shift. For zero spatial phase shift, the atoms are strongly cooled due to coherent population trapping in the given atom-field interaction scheme. On the other hand, for the case of different frequency detunings, sub-Doppler cooling of Λ atoms is possible only with a nonzero relative phase shift; it is shown that this is associated with the so-called “Sisyphus” cooling mechanism. We underscore that in our scheme neither a polarization gradient of the exciting waves nor a magnetic field is required to achieve this type of cooling pattern; two standing waves acting on different transitions of a Λ atom are sufficient. © 1994 American Institute of Physics.

1. INTRODUCTION

The behavior of different atomic systems in standing light waves has traditionally been of great interest. One such problem is the cooling of neutral atoms by a standing laser wave.^{1,2}

It is well known that the main difficulty in describing the cooling of atoms in standing waves is taking into account explicitly the microscopic spatial structure of the light field. This is manifested mathematically in the fact that the quantities determining the dynamics of an atom in a light field (force of the light pressure, momentum diffusion tensor) are continued fractions, as happened for the two-level-atom model.¹ In addition, the number of denominators of the continued fraction that must be taken into account increases with the intensity of the light waves. For this reason, such calculations are ordinarily limited to the low standing-wave intensities and different variants of the perturbation theory in the field are used, which in reality reduces to retaining only the first few denominators in the expression for the continued fraction.

Attempts to describe in this manner the interaction of a Λ atom with two standing waves were made in Refs. 3 and 4. Obviously, such an approach severely restricts the applicability of the results and does not permit investigating different effects which arise when the saturations of the transitions of the Λ atom are large.

In this paper we regard the process of cooling of Λ atoms in standing waves as being the result of the effect of the spatially homogeneous force F_z of the light pressure acting on the atoms. We derive F_z as a function of the velocities of the atoms on the basis of exact solutions for the elements of the atomic density matrix, which are represented in the form of matrix continued fractions.⁵ For this reason, in our calculations no restrictions are imposed on the ratio of the frequency detunings and intensities of the standing waves. For intense waves, we observe the existence of nonlinear multi-

photon absorption and emission effects in a three-level system, such as inversion of the light-pressure force in the region of zero velocities.^{1,2}

We emphasize that in the case of a Λ atom interacting with standing waves it is necessary to distinguish the cases of zero ($\varphi=0$) and nonzero ($\varphi\neq 0$) spatial phase shifts between the waves,^{6,7} since in the presence of such a shift the spatial structure of the field interacting with the atom is qualitatively different. We find that for $\varphi\neq 0$ and unequal detuning of the exciting waves the coefficient of dynamic friction $\partial F_z/\partial v_z$ is markedly higher and strong (sub-Doppler) cooling of the Λ atoms occurs. This can be explained by the appearance of the so-called “Sisyphus” cooling mechanism when $\varphi\neq 0$.^{8,9}

On the other hand, the “Sisyphus” mechanism no longer works when the spatial phase shift is zero ($\varphi=0$). In this case sub-Doppler cooling is observed only for two different detunings of the standing waves, and it is associated with the existence of cooling as a result of coherent population trapping in the system.¹⁰

An important part of our work is the calculation of the temperature of an ensemble of Λ atoms interacting with two standing waves. According to the theory of Brownian motion, this temperature is the ratio of the velocity diffusion coefficient and the coefficient of dynamic friction of the Λ atoms in the standing waves. We emphasize that we obtained the velocity diffusion coefficient for zero velocity of the Λ atoms taking into account the nonadiabatic corrections determined by the statistics of re-emitted photons.¹

The temperature of the cold atoms as a function of the spatial phase shift φ between the standing waves is presented in Sec. 4. The results obtained enable us to discuss the data of the experiment of Ref. 11 and to point out that this experiment involves two fundamentally different mechanisms of sub-Doppler cooling.

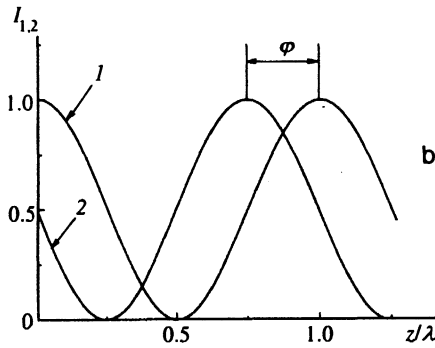
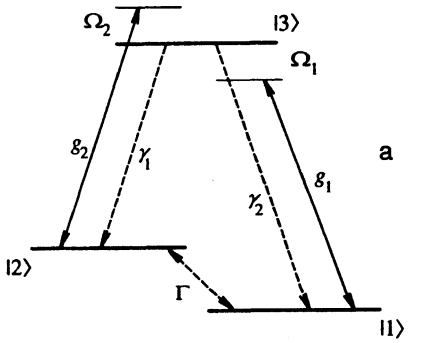


FIG. 1. a) Energy-level scheme of a Λ atom; $\Omega_m = \omega_3 - \omega_{3m}$ is the detuning of light waves with frequency ω_m from the transition frequency ω_{3m} ($m=1,2$); $2\gamma = \gamma_1 + \gamma_2$ is the total width of the upper level, where γ_m are the partial probabilities of spontaneous decays in the channels $|3\rangle \rightarrow |m\rangle$ ($m=1,2$); and Γ is the relaxation rate of the coherence between the levels $|1\rangle$ and $|2\rangle$. b) Spatial dependence of the standing-wave intensities I_m for $\varphi \neq 0$.

2. BASIC EQUATIONS

Consider a three-level Λ atom (Fig. 1a) interacting with two linearly polarized standing light waves

$$\mathbf{E}(z,t) = \mathbf{e}[E_1 \cos(\omega_1 t) \cos(k_1 z) + E_2 \cos(\omega_2 t) \cos(k_2 z + \varphi)], \quad (1)$$

where \mathbf{e} is the unit polarization vector, E_m , ω_m , and $k_m = \omega_m/c$ are, respectively, the amplitudes, frequencies, and wave vectors ($m=1,2$); and φ is the spatial phase shift between the waves (Fig. 1b). We note that the wave with frequency ω_m is resonant with the optical transition $|m\rangle \leftrightarrow |3\rangle$ of the atom and the transition $|1\rangle \leftrightarrow |2\rangle$ is dipole-forbidden.

To describe the translational motion of a Λ atom in the field (1), we employ the atomic density matrix in the Wigner representation $\rho(\mathbf{r}, \mathbf{p}, t)$. The system of equations for the elements of $\rho(\mathbf{r}, \mathbf{p}, t)$, to zeroth order in the photon momentum, has the following form:^{1,10}

$$i \frac{d}{dt} \rho_{11} = i \gamma_1 \langle \rho_{33} \rangle - g_1 (\rho_{31} - \rho_{13}) \cos(kz),$$

$$i \frac{d}{dt} \rho_{22} = i \gamma_2 \langle \rho_{33} \rangle - g_2 (\rho_{32} - \rho_{23}) \cos(kz + \varphi),$$

$$i \frac{d}{dt} \rho_{33} = g_1 (\rho_{31} - \rho_{13}) \cos(kz) + g_2 (\rho_{32} - \rho_{23}) \cos(kz + \varphi) - 2i \gamma \langle \rho_{33} \rangle,$$

$$i \frac{d}{dt} \rho_{13} = -g_1 (\rho_{33} - \rho_{11}) \cos(kz) + g_2 \rho_{12} \cos(kz + \varphi) - i \gamma \rho_{13} + \Omega_{31} \rho_{13},$$

$$i \frac{d}{dt} \rho_{23} = -g_2 (\rho_{33} - \rho_{22}) \cos(kz + \varphi) + g_1 \rho_{21} \cos(kz) + \Omega_{32} \rho_{23} - i \gamma \rho_{23},$$

$$i \frac{d}{dt} \rho_{12} = -g_1 \rho_{32} \cos(kz) + g_2 \rho_{13} \cos(kz + \varphi) - i \Gamma \rho_{12} + (\Omega_{31} - \Omega_{32}) \rho_{12}, \quad (2)$$

where $d/dt = \partial/\partial t + v_z \partial/\partial z$ is the hydrodynamic derivative; $\langle \dots \rangle$ denotes averaging over the angular distribution of the spontaneously emitted photons; $2\gamma = \gamma_1 + \gamma_2$, where γ_m are the partial probabilities of spontaneous decays in the channels $|3\rangle \rightarrow |m\rangle$ ($m=1,2$); Γ is the relaxation rate of the low-frequency coherence as a result of fluctuations of the frequencies of the optical fields or collisions of the atoms in the beam; $g_m = d_{3m} E_m / 2\hbar$ are the Rabi frequencies of the standing waves; d_{m3} are the matrix elements of the dipole moment for the transitions $|3\rangle \leftrightarrow |m\rangle$ ($m=1,2$); $\Omega_{3m} = \omega_{3m} - \omega_m$ ($m=1,2$) is the frequency detuning; and it is also assumed that the wave vectors have the same magnitudes: $|k_m| = k$.

According to Ref. 1, the force due to the light pressure can be represented in the form

$$F_z = -\hbar k [g_1 (\rho_{31} + \rho_{13}) \sin(kz) + g_2 (\rho_{23} + \rho_{32}) \sin(kz + \varphi)]. \quad (3)$$

We note that to introduce concepts such as the light-pressure force and the velocity diffusion tensor, we must impose certain conditions on the evolution time of the system and the characteristics of the atomic transitions. In our case, the first condition is

$$t \gg \gamma_m^{-1} \quad (4a)$$

and determines the times at which the system "forgets" its initial state, i.e., temporal coherence is lost. The second condition can be written in a form expressing the fact that the recoil energy $R = \hbar^2 k^2 / 2M$ of an atom is small compared to the natural linewidth $\hbar \gamma$ of the atomic transition

$$\frac{R}{\hbar \gamma} \ll 1, \quad (4b)$$

which actually means that the recoil momentum of the atom is small compared to the finite width of the velocity distribution. The conditions (4) together make it possible to use the quasiclassical approach to describe the interaction of an atomic system with the laser field.^{1,10}

We assume that the translational state of an atom changes over a characteristic time much longer than γ^{-1} (i.e., the condition (4a) holds). It can then be assumed that the elements of the density matrix are not explicitly time-dependent, but rather they are functions only of the velocity and position of an atom. For this reason, the stationary solution of the system (2) can be used to determine the light-pressure force. This corresponds formally to neglecting the partial time derivatives on the left-hand sides of the system (2) compared to the relaxation terms on the right-hand sides. In the equations thus obtained we expand the elements of the density matrix in infinite spatial Fourier series

$$\rho_{lj} = \sum_{n=-\infty}^{+\infty} \rho_{lj}^n \exp(inkz), \quad l \neq j; \quad l, j = 1, 2, 3,$$

$$\beta_m = (\rho_{33} - \rho_{mm}) = \sum_{n=-\infty}^{+\infty} \beta_m^n \exp(inkz), \quad m = 1, 2, \quad (5)$$

and then write the equations for the amplitudes of the Fourier harmonics ρ_{lj}^n and β_m^n in the form

$$\begin{aligned} inkv_z \beta_1^n &= ig_1 [(\rho_{13}^{n-1} - \rho_{31}^{n-1}) + (\rho_{13}^{n+1} - \rho_{31}^{n+1})] \\ &+ \frac{ig_2}{2} [(\rho_{23}^{n-1} - \rho_{32}^{n-1}) e^{i\varphi} + (\rho_{23}^{n+1} \\ &- \rho_{32}^{n+1}) e^{-i\varphi}] - \frac{2\gamma_1 + \gamma_2}{3} (\delta_{n,0} + \beta_1^n + \beta_2^n), \end{aligned}$$

$$\begin{aligned} inkv_z \beta_2^n &= \frac{ig_1}{2} [(\rho_{13}^{n-1} - \rho_{31}^{n-1}) + (\rho_{13}^{n+1} - \rho_{31}^{n+1})] \\ &+ ig_2 [(\rho_{23}^{n-1} - \rho_{32}^{n-1}) e^{i\varphi} (\rho_{23}^{n+1} - \rho_{32}^{n+1}) e^{-i\varphi}] \\ &- \frac{\gamma_1 + 2\gamma_2}{3} (\delta_{n,0} + \beta_1^n + \beta_2^n), \end{aligned}$$

$$\begin{aligned} inkv_z \rho_{13}^n &= \frac{ig_1}{2} [\beta_1^{n-1} + \beta_1^{n+1}] - \frac{ig_2}{2} [\rho_{12}^{n-1} e^{i\varphi} \\ &+ \rho_{12}^{n+1} e^{-i\varphi}] - (\gamma + i\Omega_{31}) \rho_{13}^n, \end{aligned}$$

$$\begin{aligned} inkv_z \rho_{31}^n &= -\frac{ig_1}{2} [\beta_1^{n-1} + \beta_1^{n+1}] + \frac{ig_2}{2} [\rho_{21}^{n-1} e^{i\varphi} \\ &+ \rho_{21}^{n+1} e^{-i\varphi}] - (\gamma - i\Omega_{31}) \rho_{31}^n, \end{aligned}$$

$$\begin{aligned} inkv_z \rho_{23}^n &= \frac{ig_2}{2} [\beta_2^{n-1} e^{i\varphi} + \beta_2^{n+1} e^{-i\varphi}] - \frac{ig_1}{2} [\rho_{21}^{n-1} \\ &+ \rho_{21}^{n+1}] - (\gamma + i\Omega_{32}) \rho_{23}^n, \end{aligned}$$

$$\begin{aligned} inkv_z \rho_{32}^n &= -\frac{ig_2}{2} [\beta_2^{n-1} e^{i\varphi} + \beta_2^{n+1} e^{-i\varphi}] + \frac{ig_1}{2} [\rho_{12}^{n-1} \\ &+ \rho_{12}^{n+1}] - (\gamma - i\Omega_{32}) \rho_{32}^n, \end{aligned}$$

$$\begin{aligned} inkv_z \rho_{12}^n &= \frac{ig_1}{2} [\rho_{32}^{n-1} + \rho_{32}^{n+1}] - \frac{ig_2}{2} [\rho_{13}^{n-1} e^{i\varphi} \\ &+ \rho_{13}^{n+1} e^{-i\varphi}] - (\Gamma + i\Omega_M) \rho_{12}^n, \end{aligned}$$

$$\begin{aligned} inkv_z \rho_{21}^n &= -\frac{ig_1}{2} [\rho_{23}^{n-1} + \rho_{23}^{n+1}] + \frac{ig_2}{2} [\rho_{31}^{n-1} e^{i\varphi} \\ &+ \rho_{31}^{n+1} e^{-i\varphi}] - (\Gamma - i\Omega_M) \rho_{21}^n, \end{aligned} \quad (6)$$

where $\Omega_M = \Omega_{31} - \Omega_{32}$, and the normalization condition $\rho_{11} + \rho_{12} + \rho_{33} = 1$ is used.

We employ the method of Ref. 5 to solve Eq. (6): We express the amplitudes of the Fourier harmonics of the off-diagonal matrix elements $\rho_{13}^{n(31)}$ and $\rho_{23}^{n(32)}$ in terms of the harmonics of the diagonal elements β_m^n ($m=1,2$) and the off-diagonal low-frequency coherence matrix elements $\rho_{12(21)}^n$. Then we obtain from Eq. (6)

$$\begin{aligned} \rho_{13}^n &= a_1^n [-g_1(\beta_1^{n-1} + \beta_1^{n+1}) + g_2(\rho_{12}^{n-1} e^{i\varphi} \\ &+ \rho_{12}^{n+1} e^{-i\varphi})], \end{aligned}$$

$$\begin{aligned} \rho_{31}^n &= b_1^n [-g_1(\beta_1^{n-1} + \beta_1^{n+1}) + g_2(\rho_{21}^{n-1} e^{i\varphi} \\ &+ \rho_{21}^{n+1} e^{-i\varphi})], \end{aligned}$$

$$\begin{aligned} \rho_{23}^n &= a_2^n [-g_2(\beta_2^{n-1} e^{i\varphi} + \beta_2^{n+1} e^{-i\varphi}) + g_1(\rho_{21}^{n-1} \\ &+ \rho_{21}^{n+1})], \end{aligned}$$

$$\begin{aligned} \rho_{32}^n &= b_2^n [-g_2(\beta_2^{n-1} e^{i\varphi} + \beta_2^{n+1} e^{-i\varphi}) + g_1(\rho_{12}^{n-1} \\ &+ \rho_{12}^{n+1})], \end{aligned} \quad (7)$$

where

$$a_m = \frac{1}{2[i\gamma - (\Omega_{3m} + nk v_z)]},$$

$$b_m = -\frac{1}{2[i\gamma + (\Omega_{3m} - nk v_z)]}, \quad (m=1,2).$$

Substituting the expressions (7) into the equations for $\rho_{12(21)}^n$ and $\beta_{1(2)}^n$ into Eq. (6) yields a system of recurrence equations that can be written as a single matrix equation

$$C_n \mathbf{x}_{n+2} + A_n \mathbf{x}_n + B_n \mathbf{x}_{n-2} = \gamma \delta_{n,0}, \quad (8)$$

where the vectors \mathbf{x}_n and $\boldsymbol{\gamma}$ have the form

$$\mathbf{x}_n = \begin{pmatrix} \beta_1^n \\ \beta_2^n \\ \rho_{12}^n \\ \rho_{21}^n \end{pmatrix}, \quad \boldsymbol{\gamma} = \begin{pmatrix} i\Gamma_1 \\ i\Gamma_2 \\ 0 \\ 0 \end{pmatrix},$$

$\Gamma_1 = (2\gamma_1 + \gamma_2)/3$, $\Gamma_2 = (\gamma_1 + 2\gamma_2)/3$, $\delta_{n,0}$ and the elements of the 4×4 matrices A_n , B_n , and C_n are given in Appendix 1.

The solution of Eq. (8) can be formally constructed as the solution of an ordinary C -number recurrence equation,⁸ in the form of an infinite fraction whose elements are 4×4 matrices obtained from A_n , B_n , and C_n :

$$\mathbf{x}_0 = \left[\begin{array}{c} A_0 - B_0 \frac{1}{A_{-2} - B_{-2}} \frac{1}{A_{-4} - B_{-4}} \frac{1}{A_{-6} - B_{-6}} \dots C_{-2} - C_0 \frac{1}{A_2 - C_2} \frac{1}{A_4 - C_4} \frac{1}{A_6 - C_6} \dots B_2 \end{array} \right]^{-1} \gamma. \quad (9)$$

The higher-order Fourier harmonics of the vector \mathbf{x} can be obtained from \mathbf{x}_0 by means of the transformations

$$\mathbf{x}_{2n} = \left(\prod_{l=0}^{n-1} T_{2l}^+ \right) \mathbf{x}_0, \quad \mathbf{x}_{-2n} = \left(\prod_{l=0}^{1-n} T_{2l}^- \right) \mathbf{x}_0.$$

Expressions for the matrices T_{2l}^\pm are presented in Appendix 1. Now the amplitudes of the Fourier components of the off-diagonal matrix elements can be determined from Eq. (7) and the light-pressure force (3) can be expressed as

$$F_z = \frac{i\hbar k}{2} \sum_{n=-\infty}^{\infty} \{g_1[(\rho_{31}^{n-1} + \rho_{13}^{n-1}) - (\rho_{31}^{n+1} + \rho_{13}^{n+1})] + g_2[(\rho_{32}^{n-1} + \rho_{23}^{n-1})\exp(i\varphi) - (\rho_{32}^{n+1} + \rho_{23}^{n+1}) \times \exp(-i\varphi)]\} \exp(inkz). \quad (10)$$

We emphasize that the force (10) can be used to describe the evolution of an arbitrary ensemble of atoms. In the important (for practical applications) case of a wide spatial atomic distribution whose width Δz is much greater than the wavelength of the light ($\Delta z \gg \lambda$), the average light-pressure force \bar{F}_z is determined only by the first nonoscillating term in Eq. (10):

$$\bar{F}_z = \frac{1}{\lambda} \int_0^\lambda F_z dz = F_z^0, \quad F_z^0 = \frac{i\hbar k}{2} \{g_1[\rho_{31}^{-1} + \rho_{13}^{-1} - \rho_{31}^1 - \rho_{13}^1] + g_2[(\rho_{32}^{-1} + \rho_{23}^{-1})\exp(i\varphi) - (\rho_{32}^1 + \rho_{23}^1)\exp(-i\varphi)]\}. \quad (11)$$

We note that the matrix-fraction method was employed in Ref. 7 to study the interaction of a V atom with standing waves and to study $J=1/2$ — $J'=1/2$ schemes of atomic levels.

3. DYNAMICS OF A Λ ATOM IN STANDING WAVES

A. Case of unequal frequency detunings $\Omega_1 \neq \Omega_2$

In the present section, we discuss the light-pressure force F_z acting on a Λ atom in standing waves with arbitrary ratios of the intensity and detuning. We emphasize that we do not consider here the case of equal frequency detuning, which will be investigated in the next section.

Figure 2a displays the force F_z obtained by the method described above in the case of low standing-wave intensities. The regions of coherent trapping, narrow structures centered on the resonant velocities

$$v_z = \pm \frac{(\Omega_1 - \Omega_2)}{2k} \quad (12)$$

are clearly seen. We note that for weak saturations of the transitions of a Λ atom, the force shown in Fig. 2a can be interpreted as being the sum of two profiles of different signs from two pairs of oppositely propagating traveling waves with different frequencies into which the field (1) can be expanded.¹⁰

Figure 2b displays the velocity distribution of a beam of Λ atoms after the beam has interacted with the standing waves. It is assumed that the beam of atoms resides in the interaction region for a time $\tau \approx 10^{-5}$ s. In the calculation, we solved the Liouville equation

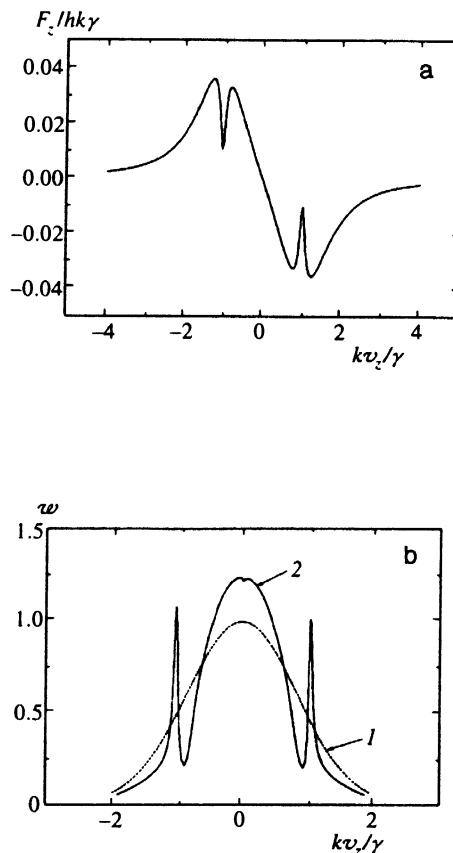


FIG. 2. a) Light-pressure force F_z acting on a Λ atom in the case of low standing-wave intensities for $\Omega_1 = -1$, $\Omega_2 = 1$, $\gamma_1 = 1$, $\gamma_2 = 0.5$, $g_1 = g_2 = g = 0.5$, $\Gamma = 0.005$, and $\varphi = 0$. b) Change introduced in the velocity distribution of Λ atoms by the force F_z from Fig. 2a. Curve 1—initial Gaussian distribution whose width corresponds to Doppler cooling; curve 2—final distribution of the Λ atoms. The interaction time is $\tau = 5\omega_R^{-1}$, where $\omega_R = \hbar k^2 / 2M$ is the recoil frequency. The two narrow peaks near the resonance values of the velocity (12) correspond to cooling of atoms as a result of coherent population trapping.⁵

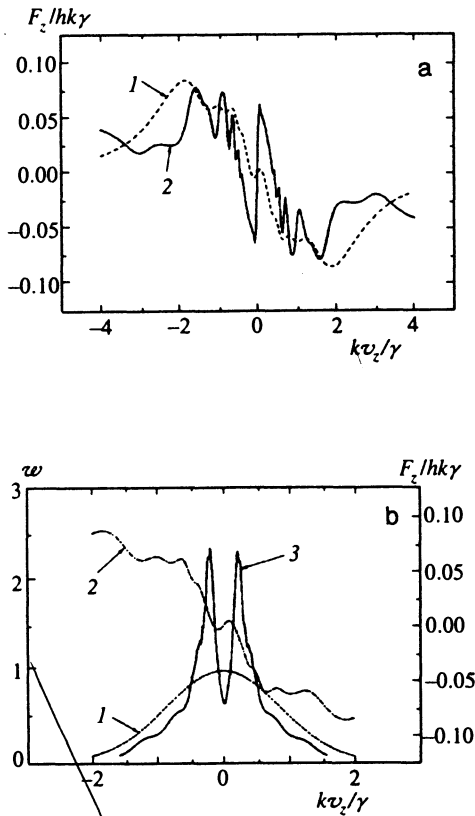


FIG. 3. a) Change in the light-pressure force F_z with increasing intensity of the standing waves. The numbers on the curves correspond to $g=1.5$ (1) and 5 (2). The remaining parameters are: $\Omega_1=-1$, $\Omega_2=1$, $\gamma_1=1$, $\gamma_2=0.5$, $\Gamma=0.005$, and $\varphi=0$. b) Velocity distribution formed by the force F_z (Fig. 3a, curve 2) over the time $\tau=5\omega_R^{-1}$. Curve 1—initial distribution; curve 2—effective force; curve 3—final distribution.

$$\frac{\partial}{\partial t} w = - \frac{\partial}{\partial p_z} (F_z w), \quad (13)$$

for the atomic distribution function $w(p)$ with the force F_z (Fig. 2a) and an initial Gaussian velocity distribution. In so doing, we assume that the broadening $(\Delta v)_{\text{dif}}$ introduced into the velocity distribution by the velocity diffusion over a time τ can be neglected.

One can see (Fig. 2b) that the velocity distribution undergoes considerable deformation over the interaction time τ only in the region of the coherent-trapping resonances (12). This is due to the high value of the coefficient of dynamic friction within the resonances (12) as compared to the value in the zero-velocity region. Correspondingly, the strong cooling of Λ atoms is likewise more efficient near the coherent-trapping resonances (12), and this makes it possible to obtain such narrow structures with effective temperatures significantly lower than the Doppler limit $T_D = \hbar \gamma / k_B$, as happened for the case of oppositely propagating traveling waves.¹⁰

The form of the light-pressure force changes qualitatively as the standing-wave intensities increase. For example, the coherent-trapping dips (Fig. 3a, curve 1) vanish, and as the intensity increases, multiphoton absorption and emission processes start to play an active role. As a result, the light-pressure force acquires a complicated multi-resonance structure, and a narrow dispersion feature appears near zero ve-

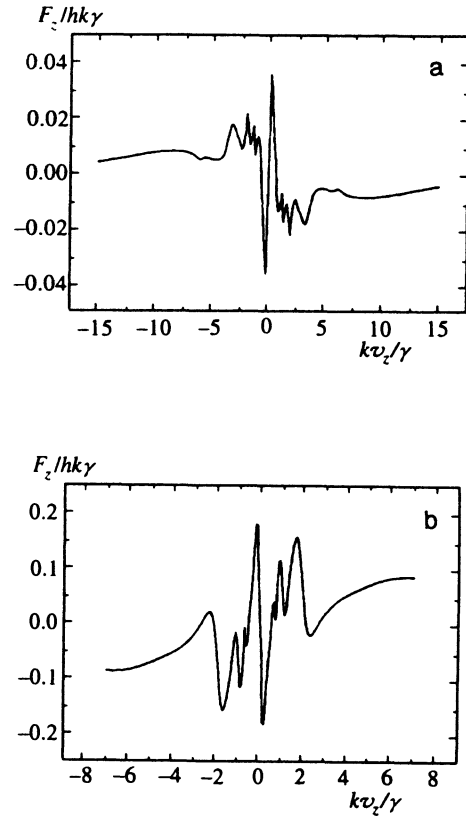


FIG. 4. Light-pressure force accompanying a change in the magnitudes and signs of the light-wave detuning. a) $g=10$, $\Omega_1=-3$, $\Omega_2=3$, $\gamma_1=1$, $\gamma_2=0.5$, $\Gamma=0.005$, $\varphi=0$. b) $g=5$, $\Omega_1=1$, $\Omega_2=2$, $\gamma_1=1$, $\gamma_2=1$, $\Gamma=0.005$, $\varphi=0$.

locity of the Λ atoms (Fig. 3a). The existence of such a structure is due to induced photon absorption and emission by Λ atoms in intense standing waves. A feature of this type in a light-pressure force is also typically present in the case when a two-level atom interacts with intense standing wave.¹ Correspondingly, the form of the velocity distribution of the Λ -atoms (Fig. 3b) after interaction with intense standing waves shows that the beam of atoms is effectively decollimated by the light field near zero velocities, while it is collimated for other values of the velocity (with the chosen values of the parameters). As a result of the combined effect of these two actions—"heating" at the center and "cooling" at the periphery—the velocity distribution of the beam of atoms acquires a characteristic "double-peak form."

It is interesting that in the case of transverse collimation of the beam of Λ atoms by two standing waves by means of an optical axicon, the distribution in Fig. 3b corresponds to a ring structure of the collimated atoms in the plane perpendicular to the propagation axis of the beam.

Finally, Figure 4 shows how the form of the light-pressure force changes when the sign and magnitude of the detuning changes in the case of large saturations of the transitions of a Λ atom. For detuning of different signs, not only does the sign of the slope of the force near zero velocities change, but additional roots also appear (Fig. 4b).

We now consider the case of nonzero spatial phase shift φ between the standing waves. We underscore that introducing a nonzero shift φ qualitatively changes the physical pic-

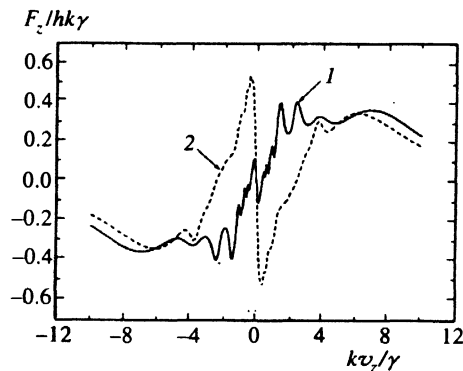
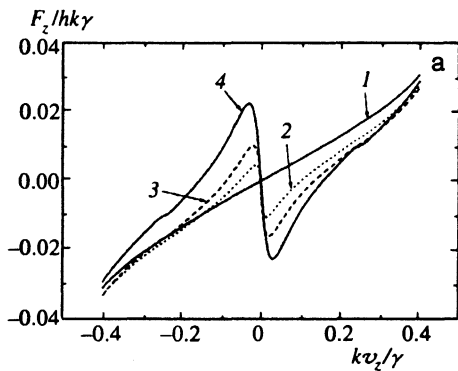


FIG. 6. Light-pressure force versus the velocity of a Λ atom in the case of intense standing waves for different values of the shift φ : $\varphi=0$ (1) and $\pi/2$ (2). The remaining parameters are: $g=5$, $\Omega_1=3$, $\Omega_2=6$, $\gamma_1=1$, $\gamma_2=1$ and $\Gamma=0.005$.

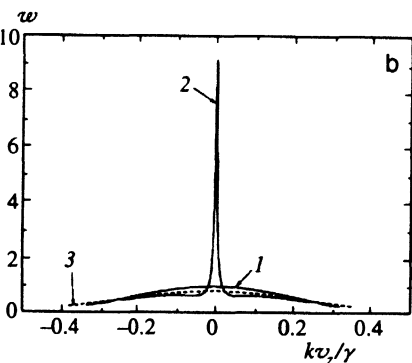


FIG. 5. a) Light-pressure force versus the velocity of the atoms for $g=0.5$, $\Omega_1=1$, $\Omega_2=2$, $\gamma_1=1$, $\gamma_2=1$, $\Gamma=0.005$ and different values of the spatial phase shift φ . The numbers on the curves correspond to $\varphi=0$ (1), $\pi/6$ (2), $\pi/4$ (3) and $\pi/2$ (4). b) Change in the velocity distribution of the Λ atoms accompanying the interaction with the field of the standing waves with $\varphi=0$ (curve 3, the interaction time $\tau=3\omega_R^{-1}$) and $\varphi=\pi/2$ (curve 2, the interaction time $\tau=1.5\omega_R^{-1}$). The initial distribution is Gaussian (curve 1). The remaining parameters are the same as in Fig. 5a.

ture of the interaction of a Λ atom with the field (1) (Fig. 1b). Indeed, in this case nonuniform optical pumping arises in the system, and as a result for low velocities of the atoms a significant fraction of the atomic population is transferred from one lower level into another. In the process, population exchange occurs between the lower levels over distances of the order of the wavelength of the light wave. Naturally, this should result in more efficient interaction of the atoms with the field than in the case of zero spatial phase shift. It is also necessary to take into account the fact that the energies of the lower levels oscillate in space in accordance with Eq. (1). This picture of the interaction between the atoms and the field for $\varphi \neq 0$ corresponds to the so-called ‘‘Sisyphus’’ cooling,⁸ which arises in combination with spatially nonuniform optical pumping and light-induced shifts of the energy levels of an atom. The cooling occurs as follows:⁸ Λ atoms in one of the lower states move in a potential produced by the periodic light-induced shift of this level. As the atoms approach the maximum of the potential, they lose kinetic energy and at the same time the probability for an atom to undergo a transition as a result of optical pumping into another unperturbed state with a smaller light-induced shift increases. With such a transition, an energy equal to the difference of the light-induced shifts of the levels at a given point

is dissipated by means of spontaneous emission. It is due to the multiple repetition of this process that the atoms slow down. This pattern of the motion of the atoms has been produced in other sub-Doppler laser cooling schemes: a polarization gradient of the exciting waves⁸ or a magnetic field.⁹ In our case, it can be achieved with two standing waves acting on different transitions of a Λ atom.^{6,7}

Figure 5a displays the light-pressure force acting on a Λ atom for different values of the spatial phase shift φ . One can see that for a shift $\varphi \neq 0$ a narrow dispersive feature appears near zero velocities of the Λ atoms. Here the slope of the force for zero velocity increases considerably, even for low values of φ . We shall show below that this results in strong (sub-Doppler) cooling of the atoms. Characteristically, the sign of the slope of the force for $\varphi \neq 0$ is different from the case of zero spatial phase shift. Correspondingly, if decollimation of the beam of atoms by the field (1) occurs for $\varphi=0$, then for $\varphi \neq 0$ beam collimation will occur for the same standing-wave detuning and intensity.

Figure 5b displays the velocity distribution of a beam of atoms for different values of the spatial phase shift after interaction with the standing waves. It is obvious that at times of order $\tau \sim \omega_R^{-1}$, where $\omega_R = \hbar k^2 / M$ is the recoil frequency and $\varphi \neq 0$ holds, an intense peak of collimated atoms forms (curve 2). On the other hand, for $\varphi=0$ the atomic beam is only weakly decollimated (curve 3).

As the intensity of the light waves increases, the form of the force F_z for $\varphi \neq 0$ changes even more dramatically (Fig. 6). For example, not only does the coefficient of friction increase, but the amplitude of the force for Λ atoms with velocity close to zero also increases and the region of velocities where the light-pressure force is determined by the value of the spatial phase shift becomes wider. We note that the characteristic velocity scale of the dispersion structure arising in the force F_z when $\varphi \neq 0$ holds depends on both the value of the spatial phase shift and the intensity of the light waves.

We have presented the change in $F_z(v_z)$ accompanying the introduction of a spatial phase shift φ for light waves with different detuning and intensity. We assumed that the

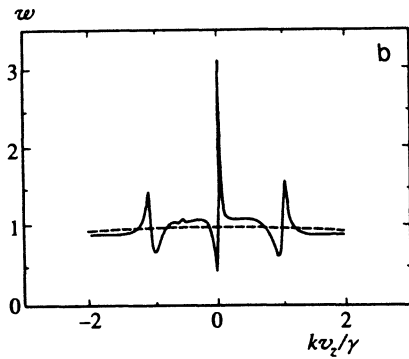
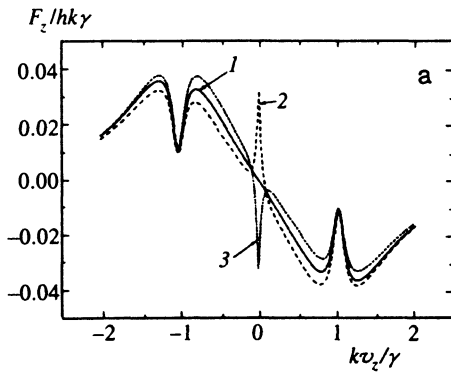


FIG. 7. a) Light-pressure force for different values of the spatial phase shift in the case of detunings of different sign. $\Omega_1=-1$, $\Omega_2=1$, $g=0.5$, $\gamma_1=1$, $\gamma_2=0.5$, and $\Gamma=0.005$. Curves: $\varphi=0$ (1), $\pi/4$ (2), and $-\pi/4$ (3). b) Change introduced in the velocity distribution by the force in Fig. 7a. The interaction time with the field is $\tau=2\omega_R^{-1}$ and the initial distribution is Gaussian (dashed curve).

frequency detuning $\Omega_{1,2}$ has the same signs. Now, let the detuning of the standing waves have different signs. Then, for $\varphi \neq 0$ a sharp peak of the light-pressure force acting on a Λ atom forms at the point $v_z=0$. The sign and amplitude of this peak are determined by the sign and the value of the spatial phase shift, and the maximum value of the amplitude is reached for $|\varphi|=\pi/4$ (Fig. 7a).

We note that this form of $F_z(v_z)$ corresponds to the presence of a “rectified gradient force” in the system.¹² Indeed, as shown in Ref. 12, such a force occurs in a Λ system if the difference between the wave vectors is large and the frequency detuning has opposite signs. Let $k_2=k_1+\Delta k$. Then $k_{2z}=k_{1z}+\Phi$, where $\Phi=\Delta kz$ is the nonuniform spatial phase shift, and the problem of excitation of the system by fields with two different wave numbers reduces to the case studied here but with a nonuniform spatial phase shift. At the same time, it is well known¹² that averaging the “oscillating rectified force” over a wavelength of the light field yields a nonzero value. For this reason, the average light-pressure force in our case is also different from zero when a Λ atom has zero velocity.

Figure 7b illustrates the change occurring in the velocity distribution of a beam of atoms under the action of the force F_z (curve 1 in Fig. 7a). One can see that there are three regions of collimation of the atoms: two peripheral regions, determined by coherent-trapping resonances (12) and a third

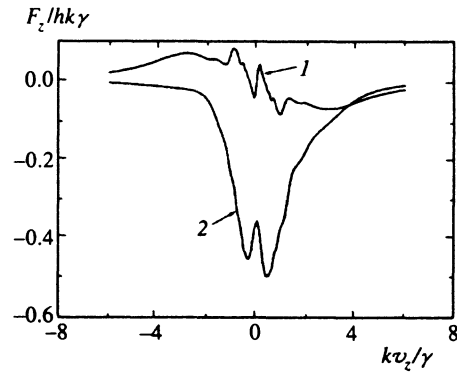


FIG. 8. Light-pressure force for different values of the spatial phase shift in the case of detuning of different sign and high standing-wave intensities. $\Omega_1=-1$, $\Omega_2=1$, $g=3$, $\gamma_1=1$, $\gamma_2=0.5$, $\Gamma=0.005$. Curves: $\varphi=0$ (1) and $\pi/4$ (2).

region on the cooling slope of the central velocity resonance of F_z . We note that in principle the effective temperature of all three peaks of collimated atoms in Fig. 7b can be significantly lower than the Doppler limit T_D .

Finally, Figure 8 illustrates the change occurring in the light-pressure force F_z in response to a change in the spatial shift φ in the case of high light-wave intensities. As one can see from the figure, the character of the velocity dependence $F_z(v_z)$ for $\varphi=0$ is completely different from the case with $\varphi=\pi/4$. For example, for $\varphi=\pi/4$ the amplitude of the force F_z increases in the region of zero velocities and the velocity interval where F_z is large becomes wider.

B. Case of equal detuning $\Omega_1=\Omega_2$

We now investigate the case in which the light waves acting on a Λ atom have equal detuning. It is well known¹⁰ that when $\Omega_1=\Omega_2$ holds coherent population trapping occurs in a Λ system. This trapping prevents excitation of the system into an upper state. Nonetheless, even for equal detuning of the standing waves

$$\Omega_1=\Omega_2=\Omega$$

a light-pressure force giving rise to strong cooling of the Λ atoms exists when the relaxation rate Γ of the low-frequency coherence between the levels $|1\rangle$ and $|2\rangle$ is taken into account.

We note immediately two circumstances that make the case of equal detuning different from the case considered above. First, relaxation (with rate Γ) of low-frequency coherence plays an important role in this situation. There are three basic physical reasons for such relaxation: fluctuations of the laser fields, transit broadening, and atomic collisions in the beam. The spectrum of the exciting fields must be quite narrow ($\Delta\omega/\omega \ll 1$), since otherwise it is meaningless to talk about the spatial structure of the light field.¹³ Second, as shown in Ref. 10, the relaxation rate of the low-frequency coherence determines the conditions which the light waves must satisfy so that the dynamics of the atoms can be described quasiclassically.

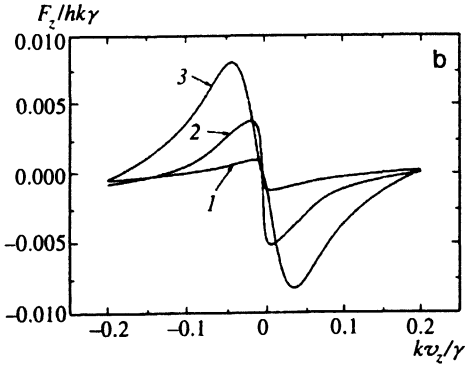
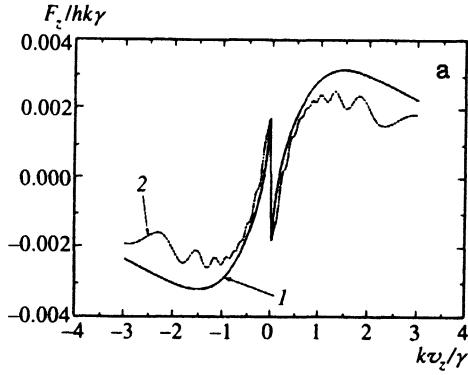


FIG. 9. a) Light-pressure force F_z versus the velocity of Λ atoms in the case of different frequency detuning: $\Omega_1=1$, $\Omega_2=1$, $\gamma_1=1$, $\gamma_2=1$, $\Gamma=0.005$, and $\varphi=0$. Curve 1—low standing-wave intensities $g=0.5$; curve 2—high standing-wave intensities $g=5$. b) Light-pressure force for different spatial phase shifts with equal detuning. $\Omega_1=1$, $\Omega_2=1$, $g_1=0.5$, $g_2=0.25$, $\gamma_1=1$, $\gamma_2=1$, $\Gamma=0.005$; curves: $\varphi=0$ (1), 0.1π (2), and $\pi/2$ (3).

Figure 9a displays the velocity dependence of the light-pressure force acting on a Λ atom when the frequency detuning of the exciting waves is equal. Obviously, in this case there is a narrow dispersive structure for Λ atoms with velocities near zero. This structure is caused not by the spatial phase shift between the standing waves, as happened previously, but rather by the characteristic manifestations of coherent population trapping in this system. Characteristically, if cooling occurs near zero velocity for the chosen values of the parameters, then even for $|v_z| \approx v_c$ (v_c is the velocity at which $F_z(v_c)=0$) cooling of the atoms by the field is replaced by heating and demochromatization of the beam occurs everywhere except for velocities $|v_z| < v_c$. Another interesting feature of this case is that as the intensity of the light waves increases, the coefficient of dynamic friction remains unchanged in the region of zero velocities (curve 2 in Fig. 9a). At the same time, for $|v_z| > v_c$ multiphoton induced absorption and emission processes appear and the light-pressure force acquires a characteristic multi-resonance structure. Multiphoton processes are not manifested in the region $|v_z| < v_c$ because they are suppressed by the coherent population trapping.

The change in the form of the force F_z accompanying a change in the spatial phase shift is shown in Fig. 9b. It is obvious that the velocity interval where monochromatization of the atomic beam is possible increases. The relatively small

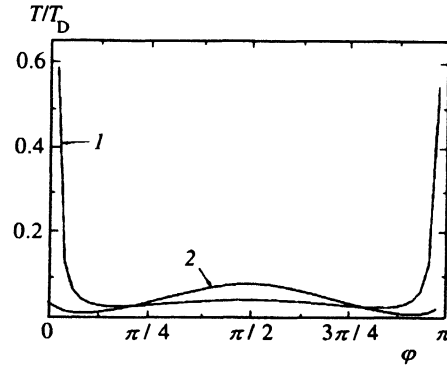


FIG. 10. Temperature of an ensemble of Λ atoms as a function of the spatial phase shift φ in the case of unequal frequency detuning $\Omega_1=1$ and $\Omega_2=2$ (curve 1) and in the case of equal detuning $\Omega_1=\Omega_2=1$ (curve 2). The remaining parameters are: $g_1=0.5$, $g_2=0.25$, $\gamma_1=1$, $\gamma_2=1$, and $\Gamma=0.005$.

change of the coefficient of dynamic friction in the region of zero velocities shows that the cooling efficiency is approximately the same for both $\varphi=0$ and $\varphi \neq 0$.

4. TEMPERATURE OF AN ENSEMBLE OF Λ ATOMS IN STANDING WAVES

In conclusion, we now study the temperature of the Λ atoms cooled in standing waves as a function of the spatial phase shift φ . To determine the temperature of the cold atoms, we calculated the velocity diffusion for zero velocity by the method of Ref. 1. Both the spontaneous and induced parts of the velocity diffusion tensor were taken into account, and the nonadiabatic correction determined by the statistics of the re-emitted photons was also taken into account in the induced part of the velocity diffusion tensor.¹ To obtain the spatial average of the momentum diffusion at the point $v_z=0$, we performed wavelength averaging of the light fields similarly to Eq. (11)

$$\bar{D}_{zz} = \frac{1}{\lambda} \int_0^\lambda D_{zz}(z) dz, \quad (14)$$

where

$$D_{zz}(z) = \hbar^2 k^2 [\gamma \rho_{33}^{(0)} + (\rho_{13}^{(1)} + \rho_{31}^{(1)}) g_1 \sin(k_1 z) + (\rho_{23}^{(1)} + \rho_{32}^{(1)}) g_2 \sin(k_2 z + \varphi)], \quad (15)$$

and $\rho_{jm}^{(0)}$ and $\rho_{jm}^{(1)}$ are the coefficients of the Wigner density matrix in the Bogolyubov series expansion:

$$\rho_{jm}(\mathbf{r}, \mathbf{p}, t) \approx \rho_{jm}^{(0)} w(\mathbf{r}, \mathbf{p}, t) + \rho_{jm}^{(1)} \hbar k \frac{\partial}{\partial p_z} w(\mathbf{r}, \mathbf{p}, t) + \dots$$

and can be found from the system presented in the Appendix 2. Then, according to the theory of Brownian motion, the temperature of the cold atoms is¹

$$T = \frac{\bar{D}_{zz}}{k_B \bar{\beta}},$$

where

$$\bar{\beta} = \frac{\partial \bar{F}_z}{\partial v_z}$$

is the average coefficient of dynamic friction, which can be obtained directly from Eq. (11).

The results of our calculations are presented in Fig. 10. One can see that for unequal detuning $\Omega_1 \neq \Omega_2$ of the light waves sub-Doppler cooling occurs in the Λ system only for $\varphi \neq 0, \pi, \dots$. As φ approaches $0, \pi, \dots$, the spatially nonuniform optical pumping vanishes and the "Sisyphus" mechanism of cooling no longer operates; it is this that results in the sharp increase of the temperature near the points $\varphi = 0, \pi, \dots$ (Fig. 10, curve 1). In contrast, for equal detuning $\Omega_1 = \Omega_2$ sub-Doppler cooling is observed irrespective of the spatial phase shift φ (Fig. 10, curve 2), since in this case cooling occurs not only by the "Sisyphus" mechanism,⁸ but also by coherent population trapping.¹⁰

From this standpoint, the experimental results of Ref. 11 on the observation of strong cooling of Λ atoms in standing waves with an arbitrary spatial phase shift are interesting. Figure 2a of Ref. 11 displays the measured profile of the atomic beam for two values of the spatial shift φ for standing waves with equal detuning. It is obvious that the quantity determining the effective temperature of the atomic beam—the width of the velocity distribution—hardly changes as the phase shift increases from 0 to $\varphi = \pi/2$, whereas the amplitude of the signal due to the cold atoms increases with the spatial shift φ . This behavior can be understood by referring to Fig. 9a, where one can see that the cooling zone $|v_z| < v_c$ increases and therefore the fraction of cooled atoms increases as the phase shift increases from $\varphi = 0$ to $\varphi = \pi/2$. On the other hand, a slight change in the width of the velocity distribution as φ changes is completely equivalent to the behavior of the effective temperature in Fig. 10 (curve 2).

We emphasize that for $\varphi = 0$, just as for $\varphi = \pi/2$, sub-Doppler cooling of the atoms occurs in the experiment of Ref. 11. In the first case cooling is due to coherent population trapping¹⁰ and in the second case the "Sisyphus" mechanism operates if there are no polarization gradients.^{6,7}

APPENDIX 1.

The elements of the matrices A_n , B_n and C_n can be written in the following form:

$$(A_n)_{11} = nk v + g_1^2(a_1^- + a_1^+ - b_1^- - b_1^+) - i\Gamma_1,$$

$$(A_n)_{12} = \frac{1}{2} g_2^2(a_2^- + a_2^+ - b_2^- - b_2^+) - i\Gamma_1,$$

$$(A_n)_{13} = g_1 g_2 \left(-a_1^- e^{-i\varphi} - a_1^+ e^{i\varphi} + \frac{1}{2} b_2^- e^{i\varphi} + \frac{1}{2} b_2^+ e^{-i\varphi} \right),$$

$$(A_n)_{14} = g_1 g_2 \left(b_1^- e^{-i\varphi} + b_1^+ e^{i\varphi} - \frac{1}{2} a_2^- e^{i\varphi} - \frac{1}{2} a_2^+ e^{-i\varphi} \right),$$

$$(A_n)_{21} = \frac{1}{2} g_1^2(a_1^- + a_1^+ - b_1^- - b_1^+) - i\Gamma_2,$$

$$(A_n)_{22} = nk v + g_2^2(a_2^- + a_2^+ - b_2^- - b_2^+) - i\Gamma_2,$$

$$(A_n)_{23} = g_1 g_2 \left(-\frac{1}{2} a_1^- e^{-i\varphi} - \frac{1}{2} a_1^+ e^{i\varphi} + b_2^- e^{i\varphi} + b_2^+ e^{-i\varphi} \right),$$

$$(A_n)_{24} = g_1 g_2 \left(\frac{1}{2} b_1^- e^{-i\varphi} + \frac{1}{2} b_1^+ e^{i\varphi} - a_2^- e^{i\varphi} - a_2^+ e^{-i\varphi} \right),$$

$$(A_n)_{31} = -\frac{1}{2} g_1 g_2 (a_1^- e^{i\varphi} + a_1^+ e^{-i\varphi}),$$

$$(A_n)_{32} = \frac{1}{2} g_1 g_2 (b_2^- e^{-i\varphi} + b_2^+ e^{i\varphi}),$$

$$(A_n)_{33} = -\frac{1}{2} g_1^2(b_2^- + b_2^+) + \frac{1}{2} g_2^2(a_1^- + a_1^+) - i\Gamma + \Omega_{21} + nk v, \quad (A_n)_{34} = 0,$$

$$(A_n)_{41} = \frac{1}{2} g_1 g_2 (b_1^- e^{i\varphi} + b_1^+ e^{-i\varphi}),$$

$$(A_n)_{42} = -\frac{1}{2} g_1 g_2 (a_2^- e^{-i\varphi} + a_2^+ e^{i\varphi}),$$

$$(A_n)_{43} = 0, \quad (A_n)_{44} = \frac{1}{2} g_1^2(a_2^- + a_2^+) - \frac{1}{2} g_2^2(b_1^- + b_1^+) - i\Gamma - \Omega_{21} + nk v,$$

$$(B_n)_{11} = g_1^2(a_1^- - b_1^-), \quad (B_n)_{12} = \frac{1}{2} g_2^2(a_2^- - b_2^-) e^{2i\varphi},$$

$$(B_n)_{13} = g_1 g_2 \left(-a_1^- + \frac{1}{2} b_2^- \right) e^{i\varphi}, \quad (B_n)_{14} = g_1 g_2 \left(b_1^- - \frac{1}{2} a_2^- \right) e^{i\varphi},$$

$$(B_n)_{21} = \frac{1}{2} g_1^2(a_1^- - b_1^-), \quad (B_n)_{22} = g_2^2(a_2^- - b_2^-) e^{2i\varphi};$$

$$(B_n)_{23} = g_1 g_2 \left(-\frac{1}{2} a_1^- + b_2^- \right) e^{i\varphi}, \quad (B_n)_{24} = g_1 g_2 \left(\frac{1}{2} b_1^- - a_2^- \right) e^{i\varphi},$$

$$(B_n)_{31} = -\frac{1}{2} g_1 g_2 a_1^- e^{i\varphi}, \quad (B_n)_{32} = \frac{1}{2} g_1 g_2 b_2^- e^{i\varphi},$$

$$(B_n)_{33} = \frac{1}{2} (g_2^2 a_1^- e^{2i\varphi} - g_1^2 b_2^-), \quad (B_n)_{34} = 0,$$

$$\begin{aligned}
(B_n)_{41} &= \frac{1}{2} g_1 g_2 b_1^- e^{i\varphi}, & (B_n)_{42} &= -\frac{1}{2} g_1 g_2 a_2^- e^{i\varphi}, \\
(B_n)_{43} &= 0, & (B_n)_{44} &= \frac{1}{2} (g_1^2 a_2^- - g_2^2 b_1^- e^{2i\varphi}), \\
(C_n)_{11} &= g_1^2 (a_1^+ - b_1^+), & (C_n)_{12} &= \frac{1}{2} g_2^2 (a_2^+ - b_2^+) e^{-2i\varphi}, \\
(C_n)_{13} &= g_1 g_2 \left(-a_1^+ + \frac{1}{2} b_2^+ \right) e^{-i\varphi}, & (C_n)_{14} &= g_1 g_2 \left(b_1^+ - \frac{1}{2} a_2^+ \right) e^{-i\varphi}, \\
(C_n)_{21} &= \frac{1}{2} g_1^2 (a_1^+ - b_1^+), & (C_n)_{22} &= g_2^2 (a_2^+ - b_2^+) e^{-2i\varphi}, \\
(C_n)_{23} &= g_1 g_2 \left(-\frac{1}{2} a_1^+ + b_2^+ \right) e^{-i\varphi}, & (C_n)_{24} &= g_1 g_2 \left(\frac{1}{2} b_1^+ - a_2^+ \right) e^{-i\varphi}, \\
(C_n)_{31} &= -\frac{1}{2} g_1 g_2 a_1^+ e^{-i\varphi}, & (C_n)_{32} &= \frac{1}{2} g_1 g_2 b_2^+ e^{-i\varphi}, \\
(C_n)_{33} &= \frac{1}{2} (g_2^2 a_1^+ e^{-2i\varphi} - g_1^2 b_2^+), & (C_n)_{34} &= 0, \\
(C_n)_{41} &= \frac{1}{2} g_1 g_2 b_1^+ e^{-i\varphi}, & (C_n)_{42} &= -\frac{1}{2} g_1 g_2 a_2^+ e^{-i\varphi}, \\
(C_n)_{43} &= 0, & (C_n)_{44} &= \frac{1}{2} (g_1^2 a_2^+ - g_2^2 b_1^+ e^{-2i\varphi}).
\end{aligned}$$

Here

$$a_m^\pm \equiv a_m^{n\pm 1} = \frac{1}{2[i\gamma - (\Omega_m + (n\pm 1)kv_z)]},$$

$$b_m^\pm \equiv b_m^{n\pm 1} = -\frac{1}{2[i\gamma + (\Omega_m - (n\pm 1)kv_z)]},$$

$$\Gamma_1 = (2\gamma_1 + \gamma_2)/3, \quad \Gamma_2 = (\gamma_1 + 2\gamma_2)/3, \quad m = 1, 2.$$

The matrices T_n^+ and T_n^- are defined as matrices relating the neighboring Fourier components of the vector \mathbf{x} :

$$\mathbf{x}_{n+2} = T_n^+ \mathbf{x}_n, \quad n > 0,$$

$$\mathbf{x}_{n-2} = T_n^- \mathbf{x}_n, \quad n < 0.$$

Recurrence relations for T_n^\pm can be derived from Eq. (8):

$$T_{n-2}^+ = -(A_n + C_n \cdot T_n^+)^{-1} B_n, \quad n > 0,$$

$$T_{n+2}^- = -(A_n + B_n \cdot T_n^-)^{-1} C_n, \quad n < 0.$$

Assuming $\mathbf{x}_{n+2} = 0$, $\mathbf{x}_{n-2} = 0$, and therefore $T_n^\pm = 0$ for some n , the matrices T can be obtained for the smaller indices, including T_0^\pm , and the vector \mathbf{x}_0 can be found [see Eq. (9)].

APPENDIX 2.

In calculating the velocity diffusion coefficient at the point $v_z = 0$, the matrix elements $\rho_{jm}^{(0)}$ can be found from the system (2) in which the derivatives satisfy

$$\frac{d\rho_{jm}}{dt} = \frac{\partial \rho_{jm}}{\partial t} + v_z \frac{\partial \rho_{jm}}{\partial t} = 0$$

and the third equation is replaced by the normalization condition

$$\rho_{11} + \rho_{22} + \rho_{33} = 1.$$

The matrix elements $\rho_{jm}^{(1)}$ are solutions of the system with the same coefficients as in the preceding case and the same vector of free terms

$$b_1 = -\rho_{11}^{(0)} f_z - g_1 \sin(kz) \operatorname{Re}(\rho_{13}^{(0)}),$$

$$b_2 = -\rho_{22}^{(0)} f_z - g_1 \sin(kz + \varphi) \operatorname{Re}(\rho_{23}^{(0)}), \quad b_3 = 0,$$

$$b_4 = -\rho_{13}^{(0)} f_z - \frac{1}{2} g_1 \sin(kz) (\rho_{33}^{(0)} + \rho_{11}^{(0)}) - \frac{1}{2} g_2 \sin(kz + \varphi) \rho_{12}^{(0)},$$

$$b_5 = -\rho_{23}^{(0)} f_z - \frac{1}{2} g_2 \sin(kz + \varphi) (\rho_{33}^{(0)} + \rho_{22}^{(0)}) - \frac{1}{2} g_1 \sin(kz) \rho_{21}^{(0)},$$

$$b_6 = -\rho_{12}^{(0)} f_z - \frac{1}{2} \sin(kz) \rho_{32}^{(0)} - \frac{1}{2} g_2 \sin(kz + \varphi) \rho_{13}^{(0)},$$

where $f_z = F_z^{(0)}/\hbar k \gamma$.

¹ V. G. Minogin and V. S. Letokhov, *Laser Light Pressure on Atoms* Gordon and Breach, New York (1987).

² A. P. Kazantsev, G. I. Surdutovich, and V. P. Yakovlev, *Mechanical Action of Light on Atoms* World Scientific, Singapore (1990).

³ Yu. V. Rozhdestvenskii, *Opt. Spektrosk.* **69**, 247 (1990) [*Opt. Spektrosk.* (USSR) **69**, 150 (1990)].

⁴ S. Chang, B. M. Garraway, V. G. Minogin, *Opt. Commun.* **77**, 19 (1990).

⁵ R. Vilaseca, G. Orriols, and L. Roso, *Appl. Phys.* **B 34**, 73 (1984).

⁶ D. V. Kosachiov and Yu. V. Rozhdestvensky, *LS SaP74, EQEC'93*, Firenze, 1993.

⁷ D. V. Kosachev and Yu. V. Rozhdestvenskii, *Pis'ma Zh. Eksp. Teor. Fiz.* **59**, 20 (1994) [*JETP Lett.* **59**, 18 (1994)]; M. S. Shahriar, P. R. Hemmer, M. Prentis *et al.*, *Phys. Rev. A* **48**, R4035 (1993); T. Cai and N. P. Bigelow, *Opt. Commun.* **104**, 175 (1993); O. Emile, C. Cohen-Tannoudji, *A. Aspect et al.*, *J. de Phys.* **2** (France) **3**, 1709 (1993).

⁸ J. Dalibard and C. Cohen-Tannoudji, *J. Opt. Soc. Am.* **B 6**, 2023 (1989).

⁹ P. van der Straten *et al.*, *Phys. Rev. A* **47**, 4160 (1993).

¹⁰ E. Korsunsky, D. Kosachiov, B. Matisov, and Yu. V. Rozhdestvensky, *Phys. Rev. A* **48**, 1419 (1993).

¹¹ R. Gupta, C. Xie, S. Padua *et al.*, *Phys. Rev. Lett.* **71**, 3087 (1993).

¹² A. Sidorov, R. Grimm, and V. Letokhov, *J. Phys.* **B 24**, 3733 (1991).

¹³ B. H. W. Hendriks and G. Nienhuis, *Phys. Rev. A* **36**, 5615 (1987).

Translated by M. E. Alferieff